

**GRAINFLOW MORPHOLOGIES AND HIGH RESOLUTION AIRFLOW MODELING OF BAGNOLD DUNES, GALE CRATER, MARS.** C. Cornwall<sup>1</sup>, M. C. Bourke<sup>2</sup>, D. W. T. Jackson<sup>1</sup>, and J. A. G. Cooper<sup>1</sup>, <sup>1</sup>Ulster University (Cromore Road, Coleraine, BT52 1SA, United Kingdom, [cornwall-c@email.ulster.ac.uk](mailto:cornwall-c@email.ulster.ac.uk), <sup>2</sup>Trinity College (Dublin, Ireland, [bourkem4@tcd.ie](mailto:bourkem4@tcd.ie)).

**Introduction:** One of the leading goals in investigating aeolian processes on Mars is to explore the boundary conditions of sediment transport, accumulation, and dune morphology in relation to wind regime as well as to quantify migration rates and sediment flux [1]. We present a qualitative and quantitative comparison between terrestrial field observations and images of preserved grainflows on the Namib dune slipface. We also investigate complex, bedform-scale wind patterns on the Namib dune that may affect grainflow magnitudes and frequencies, and ultimately influence martian dune field migration and sediment flux.

**Analysis Techniques:** A series of ground-based, high resolution laser scans with registered GPS points and video recordings were collected in the Maspalomas dune field in Gran Canaria, Spain to investigate grainflow frequency, morphology and approximate volume estimates of redistributed sediment for each type of grainflow observed (Fig. 1). Volume estimates were calculated assuming a wedge shape and inputting grainflow thicknesses and area measurements extracted from the laser scan data.

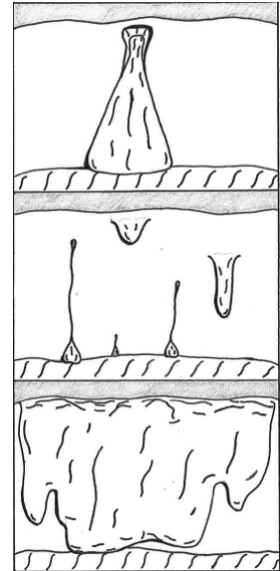
Grainflow thicknesses of a few grainflows on the Namib slipface were estimated using shadow length and the sun's elevation at the time of observation. Only grainflows with easily discernable shadows were used. Volume estimates were estimated similarly to the Maspalomas grainflows using the volume of a wedge to quantify redistributed sediment.

We investigate 3D airflow surface dynamics of the Namib dune in Gale Crater using Computational Fluid Dynamics modeling to look at the interaction between wind velocity, flow patterns and sediment transport as well as potential slope destabilization mechanisms at the bedform scale using an initial velocity of 7m/s and winds from the northeast with a kinematic viscosity of  $5.83 \times 10^{-4} \text{ m}^2\text{s}^{-1}$  to simulate average springtime conditions.

### Results:

**Earth:** Grainflow thickness ranged from 0.5mm to 7cm, generally becoming thinner upslope. Grainflow morphologies we identify are hourglass, funnel, lobe, and slab flows (Fig. 1; Fig. 2a-d). Hourglass flows were most common, initiating around 30 cm downslope from the brink and are triggered due to a localized over steepening from settling airborne sediment [e.g. 2 – 11]. These flows have been well documented in the literature and we estimate that they redistribute moderate amounts

**Figure 1. Grainflow morphologies identified on a slipface in the Maspalomas dune field, Spain including hourglass flows (top) that leave behind an alcove, minor funnel flows that transport sediment downslope through shallow, linear troughs and flattened lobe flows (middle), and slab flows (bottom) that initiated as a series of horizontal tensional cracks a few centimeters from the crest and affected large areas of the slipface.**



of sediment, averaging around  $20,000 \text{ cm}^3$  per flow. Funnels and lobe morphologies transported minor amounts of sediment and were often (but not exclusively) observed to be triggered mid-slope by minor slope instabilities likely due to return flow currents on the slipface, localized over steepening, or destabilizations in the proximity of larger grainflow events. Funnel grainflows transported sediment downslope in a shallow, linear, trough, depositing small sediment fans at the bottom of the slipface with an average volume of approximately  $1,000 \text{ cm}^3$ . Lobe flows were thin, superficial flows and rarely transported sediment to the toe of the slipface but redistributed roughly twice as much sediment as funnel flows. Slab flows were infrequent but redistributed significant amounts of sediment over a large area of the slipface averaging  $180,000 \text{ cm}^3$ , and typically spanning 5 m horizontally.

**Mars:** The Namib slipface displays a number of distinct hourglass grainflow morphologies, similar to those observed in Gran Canaria along with a few potential lobe flows (Fig. 2a and b). In contrast to field observations, the lobe flows identified on the Namib slipface tended not to form mid-slope and those that did form mid-slope appeared to initiate due to disturbances from larger hourglass flows. A series of horizontal cracks were mapped on the Namib slipface but it is unclear if these tensional cracks are similar to the ones observed in the Maspalomas slab flows.

Namib slipface grainflows were estimated to be thinner than Maspalomas grainflows, ranging from

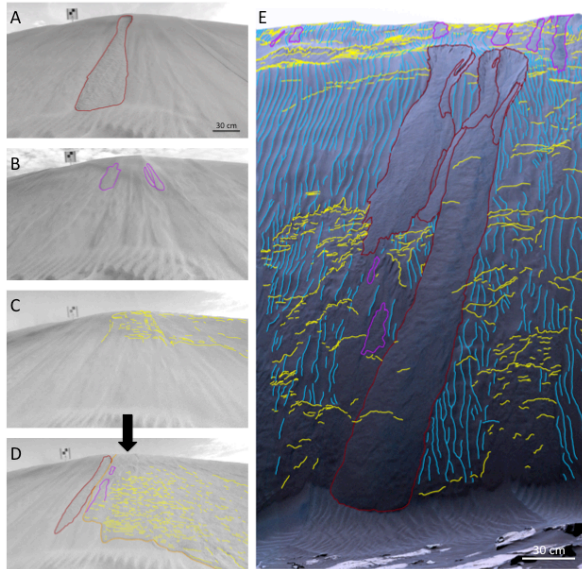


**Figure 2. Slipface morphologies from Maspalomas (A-D) and Namib dune (E). Hourglass flows are mapped in red (A and E); lobes are magenta (B and E); ripples are blue (E) and tensional cracks are mapped in yellow (C, D, and E).**

0.5mm to about 2cm. The volume of sediment estimated to be redistributed by hourglass flows on the Namib slipface ranged from about 3,000 to 25,000 cm<sup>3</sup>, comparable to some of the Maspalomas hourglass flows, while lobe grainflows only mobilized between 6 and 170cm<sup>3</sup> of sediment, significantly smaller than lobes and funnels in Maspalomas.

**CFD Results.** We are conducting an ongoing investigation into possible trigger mechanisms for the grainflows identified on the Namib slipface. We begin with a simple CFD airflow model that takes into account martian atmospheric and surface conditions. Early modeling results show airflow, displayed as color coded

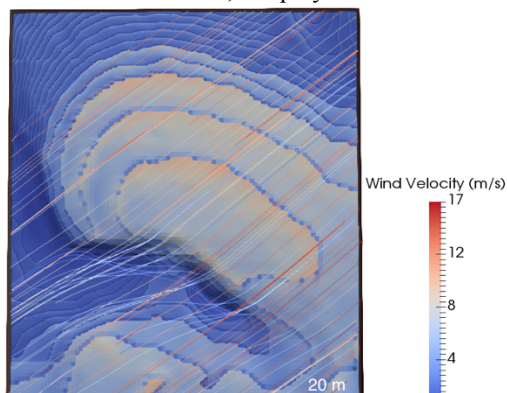


**Figure 3. Airflow modeling results for Namib dune for springtime conditions recorded by Curiosity from sol 54. Streamlines indicate airflow paths and are color coded for velocity along with the surface, where warmer colors indicate greater velocities.**

streamlines, accelerating up the stoss slope and steering effects flowing around the lee side of the dune (Fig. 3), likely resulting in the formation of the ripples seen in Figure 2. No turbulent flow on the slipface was observed in the modeling results for the specific spring-time conditions used here. We continue to investigate possible triggers for grainflow initiation on the slipface using a variety of velocities and variable seasonal wind directions.

**Conclusions:** Terrestrial studies of slipface advancement and dune migration have identified mechanisms for triggering grainflow such as lee slope destabilization due to neighboring grainflow or over steepening from grainfall accumulation [e.g. 2-11] and complex, turbulent airflow patterns on the slipface [12, 13]. In terrestrial aeolian environments, grainfall introduces new sediment on to the lee slope while complex airflow redistributes sediment across the slipface, quickly filling in alcoves and rebuilding the slope to the angle of repose until localized over steepening from grainfall triggers another grainflow. The preservation of a variety of grainflow morphologies on the Mars Namib slipface and little evidence of filled in alcoves may indicate that grainfall is not a primary mechanism in rebuilding the slipface and triggering further grainflows. More investigation of airflow currents on the slipface is needed to understand how sediment is added to and redistributed on the lee slope. We continue to investigate potential triggers for the grainflows imaged by Curiosity rover using CFD modeling.

**References:** [1] Fenton, L. K. et al. (2013) *Aeolian Res.*, 8, 29-38. [2] Bagnold, R. (1954) *Methuen*, London, 265. [3] Allen, J. (1970) *Geol.* 78, 326-351. [4] Hunter, R. (1985) *Sed.* 32(3), 409-422. [5] Anderson, R. (1988) *Sed.* 35(2) 175-188. [6] McDonald, R. and R. Anderson (1996) *J. Sed. Res.* 66(3), 642-653. [7] Nickling W. G. et al. (2002) *Sed.* 49(1), 191-209. [8] Breton, C. N. et al. (2008) *Geomorph.* 95(3-4), 518-523. [9] Sutton, S. L. F. et al. (2013) *JGR*, doi:10.1002/jgrf.20130. [10] Pelletier, J. D. et al. (2015) *JGR*, 120, 1911-1934. [11] Nield, J. M. et al. (2017) *Geol.* Doi:10.1130/G38800.1. [12] Jackson, D. W. T. et al. (2013) *J. Coastal Res.* 65, 1301-1306. [13] Cupp, K. N. et al. (2005) *AGU*, abs #H51C-0386.